

Elasticity Theory of Macromolecular Aggregates

A. Aggarwal,¹ J. Rudnick,² R. F. Bruinsma,^{2,3} and W. S. Klug^{1,3}

¹*Department of Mechanical and Aerospace Engineering, University of California, Los Angeles, California 90095, USA*

²*Department of Physics and Astronomy, University of California, Los Angeles, California 90095, USA*

³*California NanoSystems Institute, University of California, Los Angeles, California 90095, USA*

(Received 20 October 2011; published 3 October 2012)

We present a version of continuum elasticity theory applicable to aggregates of functional biomolecules at length scales comparable to that of the component molecules. Unlike classical elasticity theory, the stress and strain fields have mathematical discontinuities along the interfaces of the macromolecules, due to conformational incompatibility and large scale conformational transitions. The method is applied to the P-II to EI shape transition of the protein shell of the virus HK97. We show that protein residual stresses generated by incompatibility drive a “reverse buckling” transition from an icosahedral to a dodecahedral shape via a “critical” spherical shape, which can be identified as the P-II state.

DOI: [10.1103/PhysRevLett.109.148102](https://doi.org/10.1103/PhysRevLett.109.148102)

PACS numbers: 87.10.Pq, 46.32.+x, 87.15.bk, 87.15.hp

Continuum physics describes materials in terms of continuous fields, such as the stress and strain tensor fields of solids [1], subject to conservation laws, and linked together by constitutive relations. Whether the constituent components are atoms or small molecules, the intercomponent spacing typically determines a characteristic length scale below which continuum physics must be replaced by a discretized, atomistic description. Many of the materials important in cell biology, such as cytoskeletal protein filaments, chromatin, bacterial and plant cell walls, and lipid bilayer membranes, are aggregates assembled from thousands to millions of macromolecular components (e.g., proteins, lipids, or even cells). Continuum descriptions have been quite successful in reproducing and explaining the physical behavior of biological materials on length scales large compared to that of the components [2], but as micromechanical techniques continue to provide experimental characterization at smaller and smaller length scales, the need has grown to apply or extend continuum theories to length scales comparable to that of the constituent components. Intriguingly, because these macromolecules are themselves already large compared to atomic length scales, their mechanical function is generally determined more by gross three-dimensional shape than by atomistic-scale structure and interactions, such that coarse-grained and continuum elastic techniques have become standard tools for modeling even single proteins [3].

Despite these successes, a fundamental obstacle remains facing the application of continuum elasticity theory to protein aggregates: a protein has in general an irregular, asymmetric shape that is *incompatible* with the continuous tiling of planes or the filling of space. Elasticity theory starts from the definition of a stress-free reference state from which displacements are to be measured. Normally this state is globally compatible, meaning that the reference geometry of an elastic body can be described mathematically by a continuous position mapping. However, this

is not generally so for an aggregate of macromolecules, which need not be geometrically compatible with the final assembly state. When proteins are held together in aggregates by attractive, noncovalent protein-protein interactions, they will be deformed, necessarily producing internal “residual” stresses. Moreover, the proteins in an aggregate are functional entities, possibly active as enzymes or motor proteins, and can undergo independent conformational motions involving *large* displacements and deformations that may be *discontinuous* across protein-protein interfaces. These considerations pose a fundamental problem for elasticity theory: although the molecules may be large enough to justify a continuum description, the conformational incompatibility of the subunits renders the stress-free reference state nontrivial, and generally distinct from the experimentally observed structure.

In this Letter we outline an elastic continuum theory for aggregates of functional proteins applicable at length scales comparable to that of the proteins themselves (or larger). It differs from conventional elasticity theory in that stress and strain fields are no longer continuous functions of location: interfaces between the constituent components are lines of mathematical discontinuity in the stress and strain fields.

The method is best illustrated by a concrete example: for this we focus on the thoroughly studied bacteriophage virus HK97 [4]. The capsid of HK97 is a protein shell, surrounding a double-stranded DNA genome. It is composed of 420 identical proteins arranged in a so called “ $T = 7$ ” icosahedral lattice of 12 “pentons” and 60 “hexons” (see Fig. 1). Viral capsids are not passive containers but macromolecular machines able to perform specific tasks. In the present case, insertion of the viral genome molecule into the capsid triggers a sequence of conformational changes, known as “maturation,” that progressively strengthens the shell. The sequence initiates

with the “P-II to EI” transition [4] (see Fig. 1). Cryo-EM pictures of HK97 show that this transformation is marked by both a change in capsid shape from spherical to polyhedral and a change in the shapes of the hexons from skewed or “twisted” to symmetric (Fig. 1). Detailed x-ray reconstructions reveal that the transformation is driven by the release of elastic energy, stored in the highly deformed hexons [4]. Although later stages in maturation involve the formation of new covalent bonds among capsomers, the P-II to EI transition involves only changes in the shape or conformation of the proteins, as is more common in maturation of other viruses.

The natural stress-free equilibrium reference state is the “Caspar-Klug” (or CK) icosahedron, a perfect icosahedron, the flat facets of which are covered by twelve regular pentagons and $10T - 1$ regular hexagons [see Fig. 2(a)] for certain integer values $T = 1, 3, 4, 7, 13, \dots$ [5]. Apart from bending energy costs associated with the sharp folds of an icosahedron, the CK structure is stress free. The introduction of bending and stretching energies, according to classical elasticity theory, introduces stress and strain fields that are analytic functions of position, except at the fivefold symmetry sites, the locations of fivefold disclinations [6]. The nature of the capsid proteins enters through the values of a (two-dimensional) Young’s Modulus Y , a Poisson ratio ν , and a bending modulus κ . A “buckling transition” takes place when the Föppl–von Kármán (FvK) number $\gamma = \frac{YR^2}{\kappa}$ exceeds a critical value of the order of 10^2 . When applied to the P-II to EI transformation, the theory would describe the shape change as a buckling transition due to an increase of the FvK number across the buckling threshold. However, the in-plane displacements (skew to symmetric) of Fig. 1 do not match the predictions of the classical theory.

To account for the conformational change, the reference state for HK97 is again a collection of hexons and pentons distributed over a $T = 7$ shell; but now they are considered as if they were *isolated*. The hexons can undergo a large conformational transformation indexed by a collective reaction coordinate η : here the amplitude of hexon shear

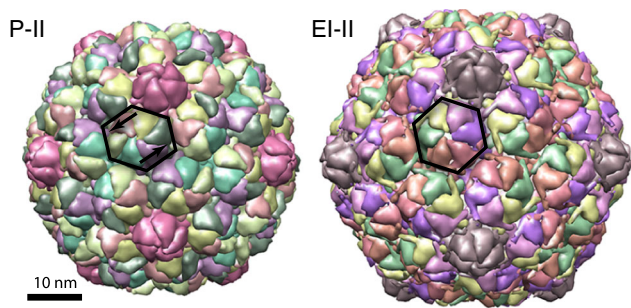


FIG. 1 (color online). Maturation of bacteriophage HK97 from “P-II” state to “EI-II” state involves “unshearing” of skewed hexons.

along a vertex-vertex symmetry direction (see Fig. 1). A constrained hexon equilibrium free energy $f_6(\eta)$, a “potential of mean force” (PMF), is assigned to the hexons. The PMF may in general be a multiwelled function depending on the detailed atomic structure of the proteins but we only need the fact that, because of the sixfold symmetry of hexons, $f_6(\eta)$ equals $f_6(-\eta)$ so $f_6(\eta = 0)$ must be an extremum. In view of the thermodynamic stability of the EI state in the absence of further chemical reactions, this extremum is an absolute minimum. The free energy difference between the EI and P-II states drives the transformation.

The method to model hexon transformation is illustrated in Fig. 2. Figure 2(a) shows a $T = 7$ shell assembled from flat, equilateral hexagons and pentagons following the CK construction. Energy minimization of the CK icosahedron partially relaxes bending at the icosahedral edges and vertices at the expense of some in-plane stretching, to yield the smooth but aspherical shape in Fig. 2(d), similar to the EI state. Note that the tiling pattern is chirally asymmetric, which will play an important role. Figure 2(b) shows what happens when the isolated hexons undergo a preshear,

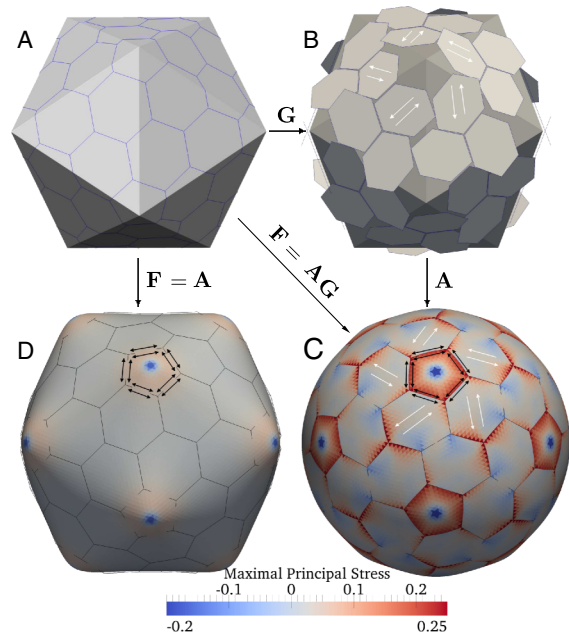


FIG. 2 (color online). Model of incompatible conformational shearing of HK97 hexons. (a) $T = 7$ icosahedral lattice. (b) Incompatible shearing of hexons ($\eta = 0.2$) by conformational deformation gradient tensor \mathbf{G} . White arrows indicate the direction of the conformational shear \hat{n} . (c) Equilibrium shape of a shell of sheared hexons ($\eta = 0.2$) for $\gamma = 2000$. Compatibility is restored by a deformation gradient tensor \mathbf{A} . Note the stress discontinuities. Black double-headed arrows indicate the principal stress direction. (d) Equilibrium shape of shell of symmetric hexons ($\eta = 0$), for which the classical theory of Ref. [6] is recovered. Note the facets and the absence of stress discontinuities.

denoted by the deformation gradient tensor \mathbf{G} , consistent with Fig. 1: it spoils the tiling. To restore the integrity of the shell, an additional deformation is introduced, denoted by the gradient tensor \mathbf{A} .

Strains in a continuum containing residual stresses due to plasticity or other forms of constitutive incompatibility may be described rationally in large-strain continuum mechanics theory by a “multiplicative split” [7] of the gradient tensor $\mathbf{F} = \nabla \vec{y} = \mathbf{A}\mathbf{G}$ of a (continuous, one-to-one) deformation mapping $\vec{y} = \vec{y}(\vec{x})$ from a position \vec{x} in the (initial, prestressed) reference configuration to a deformed position \vec{y} . Here, the conformational part of this decomposition, $\mathbf{G} = \mathbf{I} + \eta \hat{n} \otimes \hat{m}$, represents the shear of a reference hexagon with reference to orthonormal unit vectors \hat{n} and \hat{m} . As shown in Fig. 2(b), these shear directions are chosen to be compatible with that of Fig. 1. As a result of this choice, the conformational movement of the hexons constitutes a separate source for chirality. The elastic in-plane strains are described by a right Cauchy-Green deformation tensor $\mathbf{C} \equiv \mathbf{A}^T \mathbf{A}$. Accordingly, there are now *two* sources of strain: strain generated by the need to deform sheared hexons so they can tile a closed shell, and strains generated by the curvature along the edges of $T = 7$ icosahedral facets, as in the classical theory. The complete deformation (and the actual form of \mathbf{C}) from the initial state to the final state [see Fig. 2(c)] is obtained by free energy minimization. The elastic free energy associated with the mapping is then

$$\mathcal{F} = \frac{1}{2} \int dA \left[\kappa (2H)^2 + K(J-1)^2 + \mu \left(\frac{\mathbf{C}}{J} - 2 \right) \right] + 60f_6(\eta), \quad (1)$$

In the first term, κ is the bending modulus and H the mean curvature. The second and third terms account for area dilation and isochoric shear. Here, K is the two-dimensional (area) bulk modulus, $J = (\det \mathbf{C})^{1/2}$ is the deformed-to-reference area ratio, and μ is the shear modulus. The last term describes the internal energy of the hexons. In the limit of small strains with $\eta = 0$, this formulation recovers exactly the model of Ref. [6]. We note also that in the general case of a multiwelled PMF, $f_6(\eta)$, describing transitions between distinct conformational states, the effective free energy obtained by independent minimization or “static condensation” of the conformational or reference state η will be *nonlinear* in the deformation \mathbf{F} , much like the nonconvex nonlinear strain energies common for modeling martensitic phase transitions in solids [8].

Equation (1) defines a variational energy for the shell from which the deformation mapping $\vec{y} = \vec{y}(\vec{x})$ must be determined by minimization at fixed η . Constrained equilibrium configurations of the shells were computed numerically by minimizing a finite element discretization of Eq. (1) using C^0 -Lagrange interpolation for stretching energies and C^1 -conforming subdivision surface elements

for bending energies [9]. All integrals are computed over the icosahedral reference configuration of Fig. 2(a). The surface position map $\vec{y}(\vec{x})$ of the deformed shape has no discontinuities. Finally, the free energy must be minimized with respect to η to set uncompensated forces *inside* the hexons to zero.

Shells with symmetric hexons computed this way [Fig. 2(d), $\eta = 0$] reveal the smoothly varying stress distribution predicted by the classical theory: compressive stresses emanate from the icosahedral vertices, relaxing to slightly tensile values away from the pentons. The pronounced polyhedral shape of Fig. 2(d) indicates that the FvK number ($\gamma = 2000$) is well above the critical value. In contrast, Fig. 2(c) shows that preshear ($\eta = 0.2$) produces a pattern of large jumps or discontinuities in tangential stress across the capsomer interfaces. Coincident with this heterogeneous, discontinuous stress distribution, hexon preshear also produces a notable change in the shape of the shell: the shell is close to spherical [Fig. 2(c)] even though the FvK number remains well above the critical value. In other words, as a function of the hexon preshear, capsids undergo a *reverse buckling transition* at fixed FvK number.

Figure 3 illustrates a mechanism for reverse buckling. A regular pentagon is surrounded by a ring of five regular hexagons with the same edge length, all lying in a plane. Gluing together the edges between the hexagons introduces elastic stresses that can be eliminated by letting the structure buckle out of the plane. Next, shearing the hexagons along the dashed lines reduces the angular width of the gaps between the hexons and thus the elastic stresses. The geometrical construction of Fig. 3 in fact suggests that there may be a critical preshear such that there is no buckling at all.

To locate this special preshear, we show in Fig. 4 the bending and stretching energies as a function of η for $\gamma = 2000$. The stretching energy is minimized for $\eta = 0$, as would be expected, but the bending energy is minimized at a finite η . The reason becomes clear when one plots the asphericity of the shell—the normalized standard deviation of the radius—as a function of η (solid line with dots): the

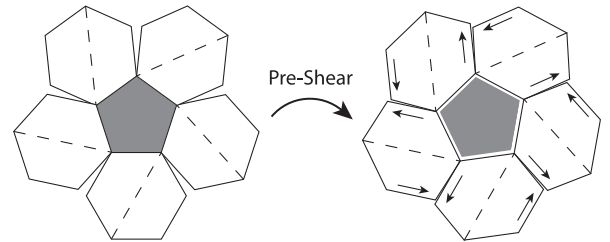


FIG. 3. Schematic showing a ring of sheared hexons surrounding a penton (gray). The shearing of the hexons both reduces the disclination angle, and elongates the hexon edges adjacent to the penton.

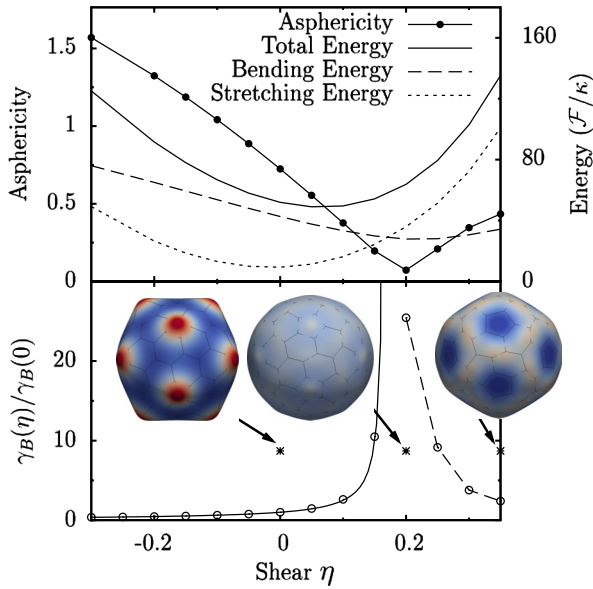


FIG. 4 (color online). Asphericity and energy vs hexon shear, η . (a) Asphericity $A = \sqrt{\langle \Delta R^2 \rangle} / \langle R \rangle$, normalized by that of an icosahedron, attains a minimum at $\eta \approx 0.2$ for $\gamma = 2000$. Total energy minimized at $\eta \approx 0.08$. (b) Shape phase diagram of shells with presheared hexons. Open circles: critical FvK number γ_B at which the shell buckles. Solid line: Eq. (2). Dashed line: interpolation. Insets: equilibrium shapes at $\eta = 0, 0.2$, and 0.35 , contoured by radius, for $\gamma = 2000$.

asphericity attains a sharp minimum value at $\eta \approx 0.2$. The capsid shape is spherical at that point [see Fig. 4(b)], which indeed is the state of minimum bending energy. The value of this special shear was found to be insensitive to changes in the elastic moduli of the shell.

What happens if η is pushed past this “critical point”? The deformed surface becomes flatter over the pentons while triangular cusps appear at the threefold symmetry sites in between the pentons. In fact, the capsid is now a dodecahedron instead of an icosahedron [see Fig. 4(b)]. The critical η thus marks a shape transition from icosahedral to dodecahedral faceting. Note from Fig. 4(a) that negative values of η produce shell shapes with a level of asphericity that exceeds that of an icosahedron. The fivefold sites are then more “spiky” than for a perfect icosahedron, resembling a stellated icosahedron.

One might speculate whether a description that includes the internal degrees of freedom and incompatibility stresses could be “coarse grained” to produce a version of the classical theory with a set of effective moduli, e.g., an effective FvK number that depends on the internal coordinate η . Since there is no icosahedral-dodecahedral transition in the classical theory, this is not possible beyond the critical point. However, below the critical point the computed capsid shapes indeed can be approximated by the classical theory if one treats the FvK number as a fitting parameter. Figure 4(b) shows the effective critical FvK number (at which the asphericity crosses the buckling

threshold) as a function of η (open circles). It increases by an order of magnitude near the critical point.

An analytical expression for such an effective FvK number can be obtained from a simplified linear analysis of Fig. 3. As described in detail in the Supplemental Material [10], we can approximate the central penton as a disk of radius $a_p < R$ and the five hexons as an annulus with radii $a_p < r < R$ surrounding the central disk. Introduction of a fivefold disclination at the center, and a hexon shear stress of amplitude η 30 degrees from radial in the annulus, has two effects: (i) the annulus expands, opening a gap along the cut, and (ii) the effective disclination angle of the annulus is reduced. Restoring compatibility by gluing back the outer annulus to the central disk along the circular cut generates a shear stress discontinuity along the cut, a slip line. An exercise in classical linear elasticity (see Supplemental Material [10]) shows that the elastic stress generated by this operation reduces the in-plane elastic energy incurred by the disclination, and produces an effective critical FvK number for buckling:

$$\gamma_B(\eta) = \left(\frac{1}{\gamma_B(0)} - \frac{5a_p^2}{11R^2} \eta \right)^{-1}. \quad (2)$$

This expression for $\gamma_B(\eta)$ is plotted as a solid line in Fig. 4(b), with $R/a_p = 2$ showing excellent agreement with values obtained from the fully nonlinear numerical analysis with our finite element model. With increased preshear the buckling transition is pushed to increasingly larger values of γ . Indeed, the theory predicts a divergence of $\gamma_B \rightarrow \infty$ as $\eta \rightarrow \eta_{\text{crit}} = R^2/24a_p^2$, independent of the elastic moduli. For $\eta \geq \eta_{\text{crit}}$ there is no buckling transition: the shell should remain spherical no matter how small the bending modulus κ . This simple theory obviously does not account for the appearance of the dodecahedral shape.

Lastly we consider minimization of the total free energy with respect to the preshear. As expected, the elastic energy has a minimum at a value of η in between the critical value and zero, (roughly $\eta \approx 0.1$, $\gamma = 2000$), because it is the sum of stretching and bending energy (solid line in Fig. 4). Note that, unlike $f_6(\eta)$, the elastic energy lacks symmetry under sign exchange of η . This is due to the chirality of the shear directions on the $T = 7$ shells. Though $f_6(\eta)$ has an absolute minimum at $\eta = 0$, the absolute minimum of the total free energy will be at a positive value of η as evident in Fig. 4. Our theory thus predicts that even in the EI state, there must be some (small) residual hexon shear. For the P-II state, experimentally found to be close to spherical, our theory makes an unambiguous prediction: the hexon preshear in the P-II state must be close to 0.2 independent of the elastic moduli of the shell. In fact, the predicted value is strikingly close to the skew observed in the crystal structures of HK97 P-II, which is in the range 0.2–0.3 [4]. It is interesting to speculate why the P-II shell is “critical.”

It follows from Fig. 4 that, at the critical point, a change in preshear from 0.2 to 0.1 changes the effective FvK number by 2 orders of magnitude. Because the critical state is sensitive to small structural changes, it sets the stage for a large conformational change in response to an external signal.

In summary, we are proposing a method for applying continuum elasticity to protein aggregates at length scales comparable to that of the protein themselves. Stress discontinuities act as slip planes, allowing for large-scale conformational incompatibility and protein motion. We show for the specific case of the P-II to EI transformation of the capsid of the bacteriophage HK97 that the generalized theory qualitatively alters the interpretation of continuum elasticity theory: the P-II spherical shell is revealed as a “critical” structure and the range of shapes encountered in the classical theory is extended to include the dodecahedron and a (quasi)stellated icosahedron.

More generally, we have shown that the inclusion of shape incompatibility and prestress are essential components of the elasticity theory of protein aggregates. To demonstrate this general point we have constructed a highly simplified model, assuming homogeneous shell thickness and material properties for the capsid proteins. Moreover we have avoided any detailed consideration of chemical reactions and/or motor activity that may be involved in driving conformational motion. While the theory we have presented can be readily applied generally to any system in which the components retain their functional identity inside the aggregate, the success of its predictions clearly relies on additional detailed information on molecular mechanisms. One essential condition is the availability of high quality structural information concerning the macromolecules, as was the case in the example we discussed here. Furthermore, the molecular dynamics simulation of more realistic models could provide specific forms of conformational PMFs, such as $f_6(\eta)$, enabling the calculation of thermodynamic properties of aggregates,

and also some understanding of the effects of structural and conformational nonuniformity.

The authors gratefully acknowledge support from NSF Grant No. DMR-1006128. W.S.K. acknowledges partial support from NSF Grant No. CMMI-0748034.

-
- [1] A. Green and W. Zerna, *Theoretical Elasticity* (Dover, New York, 2002).
 - [2] U. Seifert, *Adv. Phys.* **46**, 13 (1997); M. M. Gibbons and W. S. Klug, *J. Mater. Sci.* **42**, 8995 (2007). W. Roos, R. Bruinsma, and G. Wuite, *Nature Phys.* **6**, 733 (2010).
 - [3] M. Lu and J. Ma, *Biophys. J.* **89**, 2395 (2005); F. Tama and C. Brooks, *Annu. Rev. Biophys. Biomol. Struct.* **35**, 115 (2006); M. Bathe, *Proteins* **70**, 1595 (2008).
 - [4] J. F. Conway, W. R. Wikoff, N. Cheng, R. L. Duda, R. W. Hendrix, J. E. Johnson, and A. C. Steven, *Science* **292**, 744 (2001); K. K. Lee, L. Gan, H. Tsuruta, C. Moyer, J. F. Conway, R. L. Duda, R. W. Hendrix, A. C. Steven, and J. E. Johnson, *Structure* **16**, 1491 (2008); I. Gertsman, L. Gan, M. Guttman, K. Lee, J. A. Speir, R. L. Duda, R. W. Hendrix, E. A. Komives, and J. E. Johnson, *Nature (London)* **458**, 646 (2009).
 - [5] D. Caspar and A. Klug, in *Cold Spring Harbor Symposia on Quantitative Biology* (Cold Spring Harbor Laboratory Press, Cold Spring Harbor, NY, 1962), vol. 27, p. 1.
 - [6] J. Lidmar, L. Mirny and D. R. Nelson, *Phys. Rev. E* **68**, 051910 (2003).
 - [7] E. Lee, *J. Appl. Mech.* **36**, 1 (1969); E. Rodriguez, A. Hoger, and A. McCulloch, *J. Biomech.* **27**, 455 (1994)
 - [8] R. Abeyaratne, J. K. Knowles, and J. K., *Evolution of Phase Transitions: A Continuum Theory* (Cambridge University Press, Cambridge, England, 2006).
 - [9] F. Cirak and M. Ortiz, *Int. J. Numer. Methods Eng.* **51**, 813 (2001).
 - [10] See Supplemental Material <http://link.aps.org/supplemental/10.1103/PhysRevLett.109.148102> for a detailed discussion of the simplified analytical model resulting in Eq. (2).